

Observed interannual variability and projected scenarios of drought in the Chorotega region, Costa Rica

Melissa RÍOS-SOLANO^{1*}, A. M. DURÁN-QUESADA^{2,3,4}, C. BIRKEL⁵,
H. G. HIDALGO^{3,6}, W. CABOS⁷ and D.V. SEIN^{8,9}

¹ Posgrado en Ciencias de la Atmósfera, Escuela de Física, Universidad de Costa Rica, 2060 San José, Costa Rica.

² Escuela de Física, Universidad de Costa Rica, 2060 San José, Costa Rica.

³ Centro de Investigaciones Geofísicas, Universidad de Costa Rica, 2060 San José, Costa Rica.

⁴ Centro de Investigación en Contaminación Ambiental, Universidad de Costa Rica, 2060 San José, Costa Rica.

⁵ Departamento de Geografía y Observatorio del Agua y Cambio Global, Universidad de Costa Rica, 2060 San José, Costa Rica.

⁶ Departamento de Física Atmosférica, Océanica y Planetaria, Escuela de Física, Universidad de Costa Rica, 2060 San José, Costa Rica.

⁷ Departamento de Física, Universidad de Alcalá, Alcalá de Henares, Madrid, España.

⁸ Alfred Wegener Institute for Polar and Marine Research, Bremerhaven, Germany.

⁹ Shirshov Institute of Oceanology, Russian Academy of Sciences, Moscow, Russia.

*Corresponding author; email: mrossolano@gmail.com

Received: May 24, 2023; Accepted: December 14, 2023

RESUMEN

Los análisis del desarrollo de la sequía en la región Chorotega basados en observaciones, muestran que, a pesar de que el área es relativamente pequeña, se presenta una variabilidad espacial en la sequía agrícola. Sin embargo, la ausencia de información de radiación neta dificulta la capacidad de proporcionar estimaciones fiables de evapotranspiración (ET), afectando la evaluación de la ocurrencia de la sequía, ya que su propagación a través del sistema hidrológico es muy sensible al método de estimación de ET. La precisión de los productos satelitales del Índice de Vegetación Normalizada (NDVI, por su sigla en inglés) y la falta de información sobre riego en las áreas agrícolas limita la capacidad de establecer adecuadamente una relación entre la sequía y la respuesta de la vegetación. Con base en las observaciones, el déficit de precipitación más pronunciado ocurre entre septiembre y octubre (−100 mm en promedio), demostrando que los cambios en la circulación de gran escala son responsables de la sequía extrema en la región. Según estudios previos, El Niño-Oscilación del Sur (ENOS) modula la variabilidad de la sequía. En su fase cálida, ENSO se favorece el desarrollo de la sequía, especialmente entre agosto y octubre con correlaciones superiores a −0.6. Las proyecciones de cambio climático en los escenarios RCP4.5 y RCP8.5 sugieren una intensificación de los eventos secos en la región Chorotega a mediados de siglo, siendo la cuenca Tempisque-Bebedero la zona más afectada en términos de disminución de las precipitaciones y el calentamiento. Se proyecta un aumento de 1 °C en la temperatura media y de hasta 2 °C para la temperatura máxima y mínima para 2050, y una disminución de 400 a 800 mm en la precipitación anual en ambos escenarios.

ABSTRACT

The observation-based analysis of drought development in the Chorotega region showed that, despite the area being relatively small, agricultural drought exhibits high spatial variability across the region. However, the lack of net radiation data hinders the capacity to provide reliable estimates of evapotranspiration (ET), affecting the assessment of drought occurrence, since its propagation across the hydrological system is very sensitive to the ET estimation method. The coarse resolution of satellite-derived Normalized Difference

Vegetation Index (NDVI) products and the lack of information on irrigation in agricultural areas limits the ability to properly establish a relationship between drought and vegetation response. Based on the observations, the most prominent precipitation deficits occur between September and October (−100 mm on average), showing that changes in the large-scale circulation are responsible for the impact of severe drought in the region. In agreement with previous studies, El Niño-Southern Oscillation (ENSO) is the main modulator of the drought severity, with the warm ENSO phase favoring an enhanced drought development and its influence being more significant between August and October, displaying correlations greater than −0.6. The climate change projections under RCP4.5 and RCP8.5 scenarios suggest the intensification of drought events in the Chorotega region at mid-century, with the Tempisque-Bebedero basin being the most affected area in terms of precipitation decrease and warming. The projected scenarios correspond to an increase of 1 °C for mean temperature and more of 2 °C for minimum and maximum temperature in the 2050 horizon, as well as a decrease of 400 to 800 mm for annual precipitation under both RCPs.

Keywords: drought, evapotranspiration, vegetation, projections.

1. Introduction

Droughts are among the most damaging natural hazards given their impact on ecosystems, agriculture, human livelihood, and economic cost to society (Logar et al., 2013; Schwalm et al., 2017; Vogt et al., 2018; Meza et al., 2020). In tropical America (Stahle et al., 2016; Jiménez et al., 2021), droughts cause major disruptions for water-limited ecosystems (Castro et al., 2018; Semeraro et al., 2020), enhance the propagation of wildfires (Taufik et al., 2017) and affect agriculture (Bacon et al., 2017). They also impact water availability for human consumption (Mullin, 2020) and affect human health due to various factors including the influence of wildfires on respiratory diseases (Machado-Silva et al., 2020) and the increase of epidemics such as malaria (Gagnon et al., 2002). Drought is associated with a prolonged decrease in water availability (van Loon et al., 2016). The absence or reduction of rainfall (meteorological drought) combined with the increase in the atmospheric demand, can be sustained in time and propagate to affect other components of the hydrological system (Miralles et al., 2019). During rainfall deficit conditions, the content of soil moisture is immediately affected due to evaporation, infiltration, and root subtraction losses. As soil moisture content drops below normal-average values, an agricultural drought develops, and the decrease in the water supply for vegetation is linked to crop losses (van Loon, 2015). If such conditions persist and reach the saturated section of the soil (groundwater reservoirs) the hydrological drought is developed. As a dry event evolves, actual evapotranspiration (E_a) decreases as a function of the soil moisture content

deficit. This relationship is regulated by surface conditions such as soil moisture and aerodynamic and radiative properties but also by conditions that are specific to the vegetation cover which include root depth and regulation of stomatal conductance (Miralles et al., 2019). Vegetation under water stress exhibits a change in photosynthesis and its capacity to provide the transpiration required by the atmospheric demand. The magnitude of these changes varies depending on the specific characteristics of the ecosystems (Cooley et al., 2018).

The assessment of drought evolution is limited by the complexity of surface interactions and the role of surface-atmosphere feedback mechanisms in the system (Miralles et al., 2019). Surface conditions (e.g., vegetation and land use) play an important role both in the response of the surface to the occurrence of rainfall extremes (Anderegg et al., 2020) and the long-term changes in the behavior of extremes by means of land-atmospheric feedbacks (Diffenbaugh et al., 2005; Lemordant and Gentine, 2019).

In this feedback, E_a considers the loss of soil vapor (evaporation) and the transpiration of the plants; it also represents a complex variety of processes that are strongly connected to local conditions (Dunn and Mackay, 1995; McCabe et al., 2019). Evapotranspiration (ET) exhibits a different response to the onset and development of a dry event, that can modify the atmospheric conditions and enhance the severity of the drought (Miralles et al., 2019). ET can be considered as an aridity indicator using the variability of the ratio between precipitation (P) and potential evapotranspiration (PET) (Hidalgo et al., 2005). Given the importance of ET to link the surface and the

atmosphere in terms of the transport of energy, water, and carbon, different methods have been developed that include direct measurements (lysimeter, evaporation tank, eddy covariance systems), indirect (Thornthwaite, Hargreaves, and Penman-Monteith equations) and remote sensing (based on satellite products such as Landsat and Terra). The indirect methods are based on surface temperature or radiation as PET estimation is driven by energy, thus omitting available water on the surface (Hidalgo et al., 2005). Although other methods consider the mass balance (Chaware et al., 2017), they do not solve the issue of the influence of vegetation and soil moisture content. Penman-Monteith approximation (Monteith, 1965) is considered a relatively precise method that integrates the different processes that account for ET (Dunn and Mackay, 1995). During the development of a dry event, low relative humidity is dominant, cloudiness is reduced, and air is warm, hence a high atmospheric demand promotes surface evaporation. Those conditions, together with the precipitation deficit result in a sustained reduction of soil water content to the point in which soil moisture reaches values below the reference threshold (critical soil moisture), resulting in the evolution of a drought (Miralles et al., 2019). In addition, the water deficit also affects vegetation, because the transpiration flux is a function of soil moisture (Dunn and Mackay, 1995) and consequently the water availability for evaporation is decreased.

Sensible and latent heat changes contribute to variations in the temperature and humidity of the boundary layer and have a direct influence on cloud formation and rainfall because of the surface-atmosphere coupling. ET plays a role in the modulation of air humidity and temperature as well as cloud formation (Martens et al., 2018). Regional climate conditions and catchment characteristics influence the length and severity of dry events (van Loon and Laaha, 2015). However, the key factor in the development of drought is the soil moisture during the dry event onset, because of its attenuation capacity (van Loon and van Lanen, 2012) and potential to affect the environmental conditions by means of surface and evaporation fluxes to the atmosphere (Koster et al., 2004), particularly in the drylands. Furthermore, soil moisture is strongly linked to the health and dynamics of the vegetation (Ji and Peters, 2003) given its capacity to regulate the stomatal conductance

and transpiration flux (Cooley et al., 2018; Miralles et al., 2019). In this regard, vegetation is integrated within the surface-atmosphere feedback component of the soil-plant-atmosphere continuum (SPAC), with variability and phenology as constraints of the energy and water fluxes (Green et al., 2017). Hence, radiative, hydraulic, and aerodynamic properties are fundamental in the response and resilience of the ecosystem to the development of dry conditions (Miralles et al., 2019).

Albeit warming scenarios suggest the likely increase of precipitation extremes, the regional and local processes that may modulate the severity and frequency of extremes and their impacts in the region are not fully understood. For small areas with complex terrain, the assessment of extreme precipitation trends is influenced by processes at smaller scales than those obtained in the global and regional climate models (Bador et al., 2020), therefore is largely dependent on observations. Such is the case for Costa Rica, for which the impact of climate variability is different for the Caribbean and the eastern tropical Pacific basins, and the mountain range system largely influences the spatial distribution of precipitation and its extremes. Embedded in the heterogeneity of precipitation across Central America, the Chorotega region, located in the northwestern portion of Costa Rica is the driest area in the country and the southernmost component of the Central American Dry Corridor (CADC) (van der Zee et al., 2012; Hidalgo et al. 2019), as shown in Figure 1. The low-frequency variability of drought is modulated by climate indices (Özger et al., 2009) from which El Niño-Southern Oscillation (ENSO) is known to dominate the signal of drought development across the globe (Vicente-Serrano et al., 2011).

Based on historical available records, droughts in the Chorotega region have been documented as early as 1922. Casanova (1993) developed the mapping of drought-prone regions to support land use management. Using precipitation records, his work estimated potential evaporation, highlighting the areas within the Chorotega region with annual precipitation below 1000 mm as the most vulnerable to drought. A positive trend (1973-2003) in the frequency and severity of drought events was identified by Birkel and Demuth (2006) using observational records. According to estimates of the Agricultural Sector Committee of Costa Rica (InfoAgro, 2015),

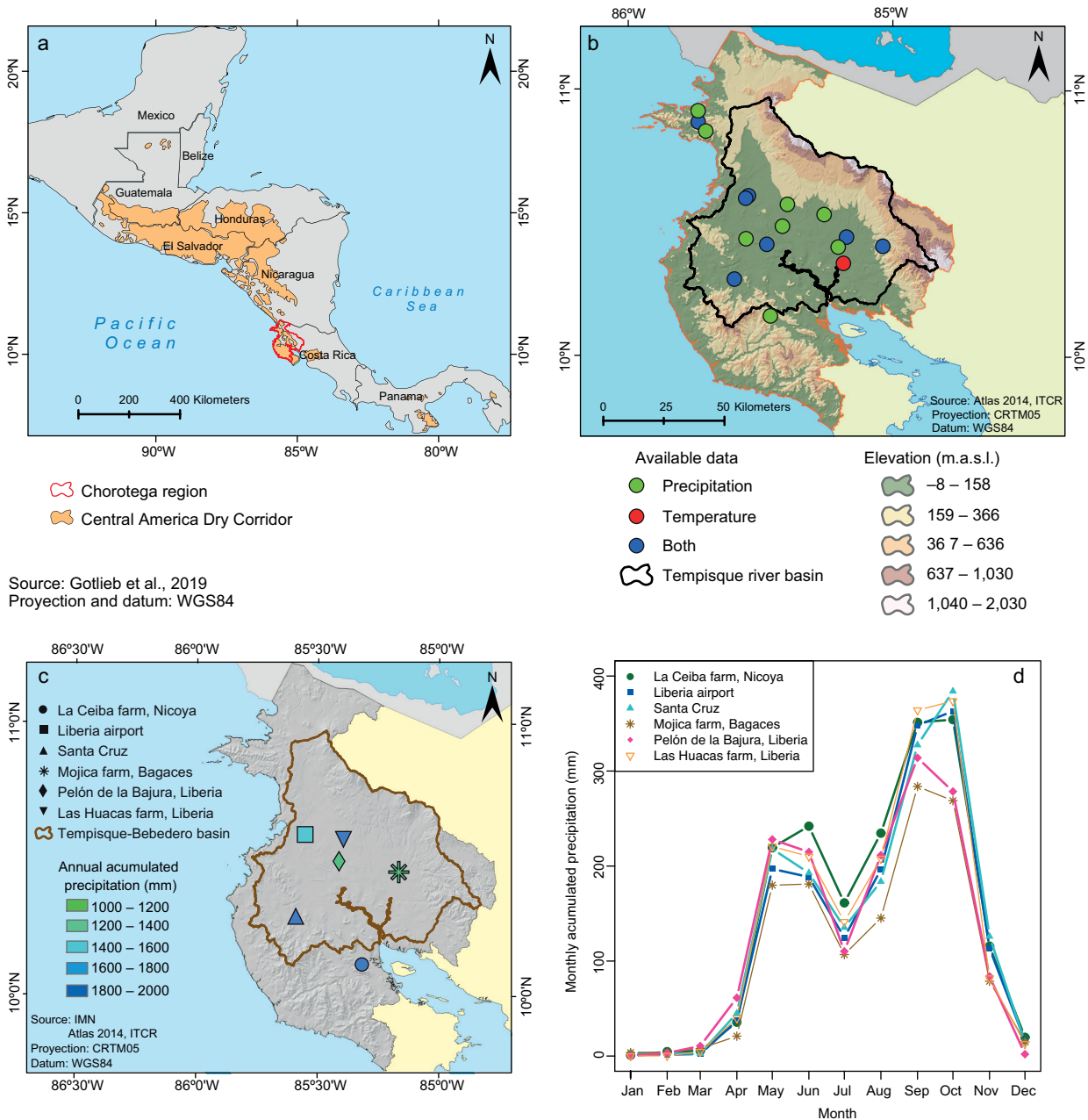


Fig. 1. (a) Location of the Chorotega region (red) within the spatial distribution of the CADC; (b) location of available long-term meteorological records for precipitation (green), temperature (red), temperature and precipitation (blue) for the Chorotega region showing topography; (c) long-term annual accumulated precipitation based on the observational records for the available stations that met the criteria for climate basis analysis, and (d) long-term mean annual cycle of precipitation for selected stations that shows the bimodal distribution that characterized rainfall and relatively homogeneity of rainfall across the Chorotega region.

drought caused nearly 26.71 million USD loss on average per year during the 2005-2011 period. During warm ENSO phases, the region experienced

the most severe dry events (Coto, 2016) given the delay in the establishment of the rainy season and the significant precipitation deficit associated with

these events. During the occurrence of dry events, agricultural production decreases, which generates severe economic damage to the region with the associated reduction in agricultural goods exports and an increase in unemployment. At the ecological level, droughts are associated with conditions that favor the propagation of wildfires, which are among the main threats to the dry forest (Campos-Vargas and Vargas-Sanabria, 2021) and are known to be severe in Guanacaste (Rozario et al., 2018). Due to the impacts of drought on the region, the study of drought development and propagation is key. Advances in the study of drought in the region include the analysis of aridity trends in Central America (Alfaro-Córdoba et al., 2020) and the role of precursors for dry spells in the CADC (Hidalgo et al., 2019).

The assessment of drought duration, severity, and propagation in complex terrain regions like Costa Rica is often hindered by the availability of long-term high-quality data. Recent studies show that although internal climate variability dominates the signal of drought in Central America, the rainfall deficit of the 2015-2019 event was likely exacerbated by anthropogenic climate change (Pascale et al., 2021), highlighting the need for improving the capacity of climate change attribution studies. The likely amplification of extreme precipitation events under warming climate conditions (Mukherjee et al., 2018; Thackeray et al., 2022) and known biases in the observational evidence of extreme precipitation trends in tropical areas address the need for regional analysis to assess the impacts of climate variability and change on drought in climate change hotspots.

This work explores the behavior of drought events in the Chorotega region based on historical records and evaluates the potential for drought development under warming conditions, providing information that can be useful to support water resources management and policy-making. The analysis explores the observed influence of precipitation deficit for drought development based on historical long-term records to determine the occurrence of meteorological and agricultural drought in the region and evaluates the impact of PET estimates in the evaluation of agricultural drought distribution. Based on the historical observations, the impact of ENSO on drought development, intensity, and spatial distribution is studied.

Based on dynamical downscaled (Sein et al., 2015) ocean-coupled simulations from research by Cabos et al., (2019), projected drought behavior is analyzed for future climate scenarios under Representative Concentration Pathways (RCPs) 4.5 and 8.5.

2. Data and methods

2.1 Study site description

The Chorotega region is located in the northwestern Pacific coast of Costa Rica and is characterized by a heterogeneous terrain composed of the Guanacaste Volcanic Range to the east and lowlands to the west that border the eastern tropical Pacific (Mora and Portuguez, 2012). Figure 1a shows the location of the Chorotega region in the context of the Central American region and its location within the delimitation of the CADC. The extension of the Chorotega region is 10 140 km² and its climate is classified as dry tropical or savannah according to the Koppen-Geiger classification (Vargas, 2006). The Chorotega region is the warmest in the country, with mean temperature varying between 26 and 29 °C on average, while mean temperature has a relatively steady behavior during the year. The diurnal temperature range (DTR) (difference between maximum and minimum temperature) has a marked seasonality, varying between 6 and 12 °C during the dry season. The Chorotega region is also the driest area of Costa Rica albeit rainfall ranges between 1200-1700 mm year⁻¹, with a heterogeneous distribution that shows lower values for the central plains and higher accumulated rainfall for stations near the Guanacaste Volcanic Range to the north and the mountain system in the Nicoya Peninsula, as shown in Figure 1c based on observational records. The annual distribution of rainfall is bimodal, with a marked dry season between mid-November to April, the rainy season established between May to November, and a relative minimum between July and August, as shown in Figure 1d. This reduction in rainfall is part of a characteristic pattern of Central American rainfall which is more pronounced in the Pacific, known as the mid-summer drought (MSD) (Magaña et al., 1999; García-Franco et al., 2022; Maurer et al., 2022) and locally as veranillo or canícula (Alfaro, 2014). The duration and intensity of the MSD is subject to inter-annual variability significantly modulated by ENSO (Ramírez, 1983; Maldonado et al., 2016); therefore,

ENSO impinges its signal on the regional rainfall patterns (Durán-Quesada et al., 2020). More specifically, during a warm (cold) phase of ENSO, regional rainfall is reduced (increased) in the Pacific slope of Central America (Amador et al., 2016).

The Chorotega region is witness to drastic changes due to the fast conversion from a traditional agricultural to a services economy, which has caused significant socioeconomic and landscape transformations with results that are not always positive (González and Vilaboa, 2010). Currently, nearly 58% of the surface (592 642 ha) is dedicated to agriculture and cattle raising, being considered one of the most productive regions in Costa Rica regarding those sectors (Hernández, n.d.). Land use changes due to the introduction of new crops, cattle raising expansion, and urban and touristic infrastructure development replaced most of the natural vegetation cover with pastures, crops, and impermeable surfaces, creating a fragmented landscape and degraded environment, causing major impacts on water resources (Ramírez and Jiménez, 1998). The latter is linked to the over-exploitation of the environment, which adds pressure under heavy rainfall and drought events and is evidenced in the decrease in surface and groundwater water reservoirs (Ramírez and Jiménez, 1998). The dependency of agricultural activities represents one of the main challenges in the region with the stability of the sector and its productivity being a major concern due to their sensitivity to weather and climate.

2.2 Data

2.2.1 Precipitation and temperature

Long-term observations from the Costa Rican National Meteorological Institute (IMN) available for the Chorotega region were used. Information from a total of 28 combined manual and automated meteorological stations was processed with records having a variable length spanning from 1938 to 2019. From the database, only stations with less than 20% of missing data were considered, hence 19 stations for precipitation and 11 for temperature were used. Because of the scarcity of nearby stations to ensure homogeneity, no data-filling procedures were used. Although some stations have longer records, the common period for the selected stations was set as 1999–2019, which ensured data availability for most of the stations within the same period.

Ocean coupled climate projections based on RCP4.5 and RCP8.5 scenarios, used for the evaluation of future drought development under warming conditions, correspond to simulations developed by Cabos et al. (2019) using the coupled regional ocean modeling (ROM) system (Sein et al., 2015). In ROM, the hydrostatic model REMO (Jacob et al., 2001), which is the atmospheric component, is coupled with the global ocean model MPIOM (Marsland et al., 2002) using the OASIS coupler (Valcke, 2013). The horizontal resolution of the simulations herein used is 50 km with CMIP5 MPI-ESM as boundary conditions. Statistical downscaling was applied to the 50 km output from the coupled system to obtain a 10 km horizontal resolution derived product, for which a validation, using observations from IMN, was conducted for the historical run (1980–2005). A homogeneity test was not implemented for this case given the amount of available nearby stations is very limited.

2.2.2 ENSO indices

Two indices representative for ENSO were retrieved from the NOAA Earth Science Research Laboratory's Physical Science Division (ESRL PSD) database, namely the Multivariate ENSO Index (MEI) (Wolter and Timlin, 1993, 1998) and Niño 3.4. The MEI is a bi-monthly index that combines information of sea level pressure, sea surface temperature (SST), wind and outgoing long-wave radiation. El Niño 3.4 index corresponds to the SST anomaly in the region enclosed by 5 N–5 S and 120–170 W.

2.2.3 Normalized Difference Vegetation Index (NDVI)

NDVI is an indicative of plant greenness in which the reflectivity of the surface is normalized, and negative values refer to water bodies (Meneses-Tovar, 2011). It enables to distinguish periods in which crops and vegetation in general present substantial losses of biomass. Among the available NDVI products, the Moderate Resolution Imaging Spectroradiometer aboard the Terra satellite (MODIS/Terra) (MOD13C2), derived from the National Oceanic and Atmospheric Administration (NOAA) Advanced Very High-Resolution Radiometer (AVHRR). The product has monthly temporal resolution at 0.05° spatial resolution. In this product, clouds are replaced

with registered climatology from MODIS to obtain a cloud-free product.

2.3. Methods

2.3.1 Estimation of evapotranspiration (ET)

Monthly temperature was used to compute reference evapotranspiration (ET_0) based on the Hargreaves (Hargreaves, 1994) approximation, given that wind and radiation information are not available for most of the stations.

$$ET_0 = 0.0023 * RA * (T_{c} + 17.8) * TD^{0.50} \quad (1)$$

The Hargreaves estimation was proposed as an alternative to the measurement of ET_0 using extra-terrestrial radiation (RA), the difference between maximum and minimum mean temperature (TD) and the average of maximum and minimum temperatures (T_c). The estimates are based on monthly scales and radiation is computed as a function of latitude (Maidment, 1993). The SPEI R library was used to compute ET_0 . For those stations for which more variables were available, ET_0 was estimated using the Penman-Monteith approximation following Dunn and Mackay (1995) and performing a correction of the radiation information using the approximation based on Julian day.

$$E_a = \frac{Rn \Delta + \frac{\rho C_p \delta_e}{r_a}}{\lambda \left[\Delta + \gamma (1 + r_s / r_a) \right]} \quad (2)$$

where Rn is the net radiation ($W m^{-2}$); ρ the air density ($kg m^{-3}$); C_p the air specific heat at constant pressure ($J kg^{-1} ^\circ C^{-1}$); δ_e the vapor pressure deficit (mbar); Δ the saturated vapor pressure gradient ($mbar ^\circ C^{-1}$); γ the psychrometric constant ($mbar ^\circ C^{-1}$); λ the vaporization latent heat ($J kg^{-1}$); r_a the aerodynamic resistance ($s m^{-1}$), that is a function of $208 U_2^{-1}$ where U_2 is the wind speed at 2-m height, and r_s is the surface resistance ($s m^{-1}$) and depends on the leaf area (Dunn and Mackay, 1995). Due to the lack of data availability, the reference value of $50 s m^{-1}$ was used for r_a , while the value used for r_s was $69 s m^{-1}$. The meteorological stations are in farmland areas mostly dedicated to cattle grazing, so the soils are dominantly covered by grass and the simplification of $Kc \sim 1$ is considered so that $Ea \cong ET_0$ and the

estimation based on the above-mentioned constants is considered valid.

2.3.2 Drought indices

Daily historical records were used to construct monthly values, which were used to compute the Standardized Precipitation Evapotranspiration Index (SPEI). SPEI is an indirect method developed to evaluate drought. It relates the monthly climate balance (difference between precipitation and ET water) as a measurement of the deficit or surplus of water. The evaluation of SPEI allows the use of different timescales, enabling the analysis of the length and propagation of drought across the hydrological system (Vicente- Serrano, et al., 2010). SPEI R library was used for the estimation of the index, previous consideration of the monthly climate balance as input for the estimation. The index was estimated for 1, 2, 3, 6, 9, and 12 months.

The Standardized Precipitation Index (SPI) (McKee et al., 1993), which determines dry periods based on rainfall deficits, was also estimated. The historical precipitation records were adjusted to a normal probability distribution in which zero corresponds to the normal or average value and negative (positive) values indicate dry (wet) periods. The estimates on different time scales reflect the impact of drought on surface water availability in short time scales and in longer time scales. SPI values are grouped into seven categories (see Table SI in the supplementary material) and the SPEI R library was also used for the estimation. In this case, time scales between three and 36 months at three-month intervals were the ranges used for the estimation of SPI. The procedure described by López-Moreno et al. (2009) was followed, with SPEI at 12 months instead of SPI, and applied to the monthly scale precipitation and temperature projections from Cabos et al. (2019) to assess future drought under warming scenarios.

3. Drought events and ENSO impact based on historical observations

3.1 Evapotranspiration

ET_0 was estimated using the Hargreaves and Penman-Monteith methods; due to the weight of extra-terrestrial radiation data in the Hargreaves equation, estimates are almost uniform throughout the year.

Because long-term records are often limited to precipitation and temperature information, estimations that include wind and radiation do not often exist. In a water-limited environment, as is the case for semi-arid regions, an increase in rainfall is associated with larger latent heat fluxes due to the increase in moisture and a decrease in the shortwave radiation due to increasing cloudiness and moisture (Donohue et al., 2010). During the dry season, ET_0 is lower due to the influence of reduced water availability and lower surface temperature as less cloudiness enables larger portions of long-wave radiation to escape back to space. As the transition from the dry to the wet season is established, ET_0 peaks. Based on the estimations for the Chorotega region stations, differences close to $100 \text{ mm month}^{-1}$ were identified between Hargreaves and Penman-Monteith estimates during the rainy season. Such differences may be associated with the limitation of Hargreaves estimation as it neglects the cloudiness conditions typical of the rainy season and consequently the humidity profiles. The Hargreaves-based estimation shows an overestimation of ET_0 compared to Penman-Monteith results. Penman-Monteith estimates of ET_0 presented in Figure 2 show maximum values between November and April coinciding with the

drier months over the Pacific slope with a peak in March ($\sim 113 \text{ mm month}^{-1}$).

From May to November, the atmospheric evaporation potential is reduced, partially due to the increase in cloudiness which limits the amount of incoming solar radiation. As a result, the energy required to increase the amount of water vapor decreases and ET_0 slightly increases during the MSD, and minimum values are observed during June ($\sim 44 \text{ mm month}^{-1}$) and September ($\sim 31 \text{ mm}$). In the context of drought dynamics, ET_0 importance lies in the energy feedback represented by latent heat fluxes and the transfer of water in the form of vapor which contributes to warming the surface (Liu et al., 2014). High temperatures are associated with increases in PET, the consequent loss of soil moisture, and a likely decrease in precipitation (Rind et al., 1990). Hence, understanding the behavior of ET and its response to climate variability and warming scenarios is fundamental to better assess drought occurrence and impacts in the Chorotega region, which is part of the CADC.

3.2 Observed drought

The identification of meteorological drought based on SPI accounts for a total of 117 events in the 1998-2019 period as shown in Figure 3a. The identification

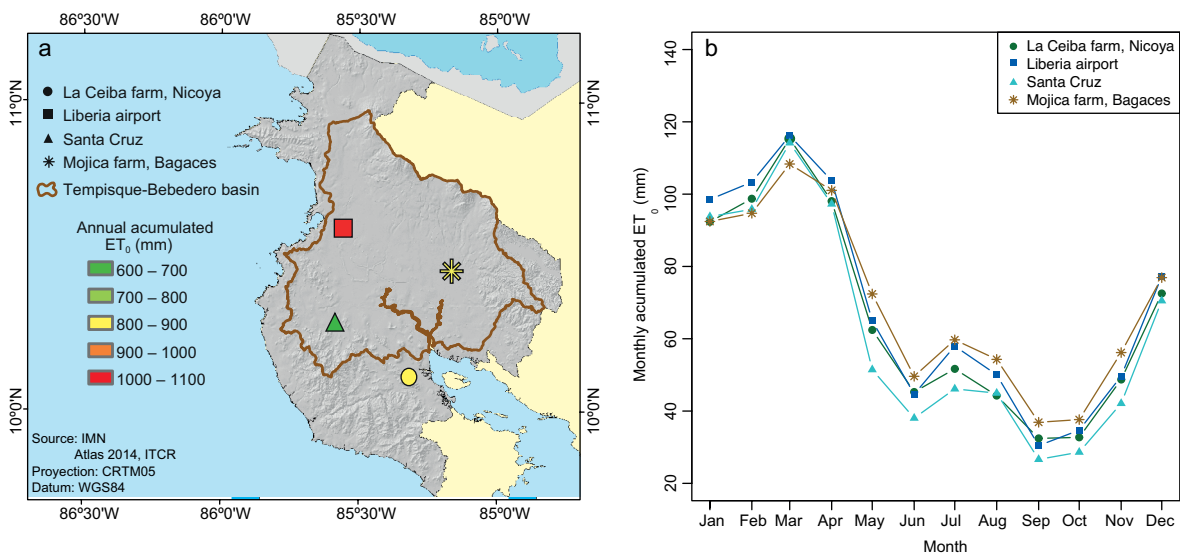


Fig. 2. (a) Annual average accumulated ET_0 over the Chorotega region, and (b) annual cycle of ET_0 , both for the period 1999-2019 based on estimates computed using the Penman-Monteith equation. The station with the highest accumulated values is in Liberia, reflecting the difference between the rainy season (lowest values) and the dry season (highest values) in relation to radiation input and cloud cover.

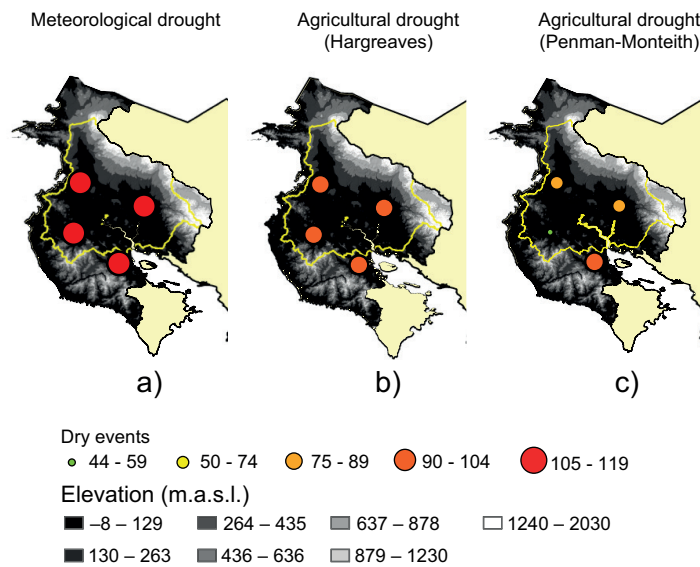


Fig. 3. Number of meteorological drought events (left) based on the SPI (the threshold value selected was zero), and agricultural drought based on the SPEI with ET_0 data estimated with the Hargreaves equation (center) and the Penman-Monteith equation (right) from 1998 to 2019. The hydrological drought presents a similar behavior to the meteorological drought and without difference between the seasons when the energy-based Hargreaves ET_0 is used.

of agricultural drought was based on SPEI and as previously mentioned, the quantification of events is sensitive to the method used to estimate ET. Using Hargreaves, a total of 102 events (Fig. 3b) were identified while fewer events were identified using Penman-Monteith, which opposite to the Hargreaves-based estimate captured the spatial variability of agricultural drought (Fig. 3c). The Gulf of Nicoya region is affected by a larger number of dry events (92) compared to Liberia (79) and Bagaces (89), while for Santa Cruz the number of identified dry events is 44, nearly half of the events identified using the Hargreaves estimation.

Albeit relevant to assessing the impact of dry extremes, the identification of meteorological drought is limited if the information required for planning and decision-making corresponds to drought propagation. In such cases, the use of SPI is limited to identifying drought events related to the increase in atmospheric demand as it only considers changes in precipitation (Vicente-Serrano et al., 2014). Given the nature of differences in the estimation of ET and their implications for the estimation of SPEI, the

identification of meteorological drought is biased depending on the implemented method to estimate ET. While this is a known general fact, it is worth highlighting in the context of the Chorotega region because, despite its relatively small size and low elevation conditions, the establishment of meteorological drought is shown to be heterogeneous. The latter is relevant for decision-making, early warning, and monitoring because the representativity of currently available meteorological stations may not properly reflect the spatial variability of drought propagation.

During the first half of the analysis period, drought indices suggest drought events to be milder compared to 2009-2010, while during the second half, SPEI values tend to be more negative and larger in magnitude (Fig. 4), consistent with the years in which more intense and prolonged drought events are observed. The shift to negative SPEI values for the Nicoya Peninsula follows the severe drought event that affected the region between 2012 and 2015 (Fig. 4a) Such was the case of Liberia with the most severe events identified for 2008 and between 2014-2016

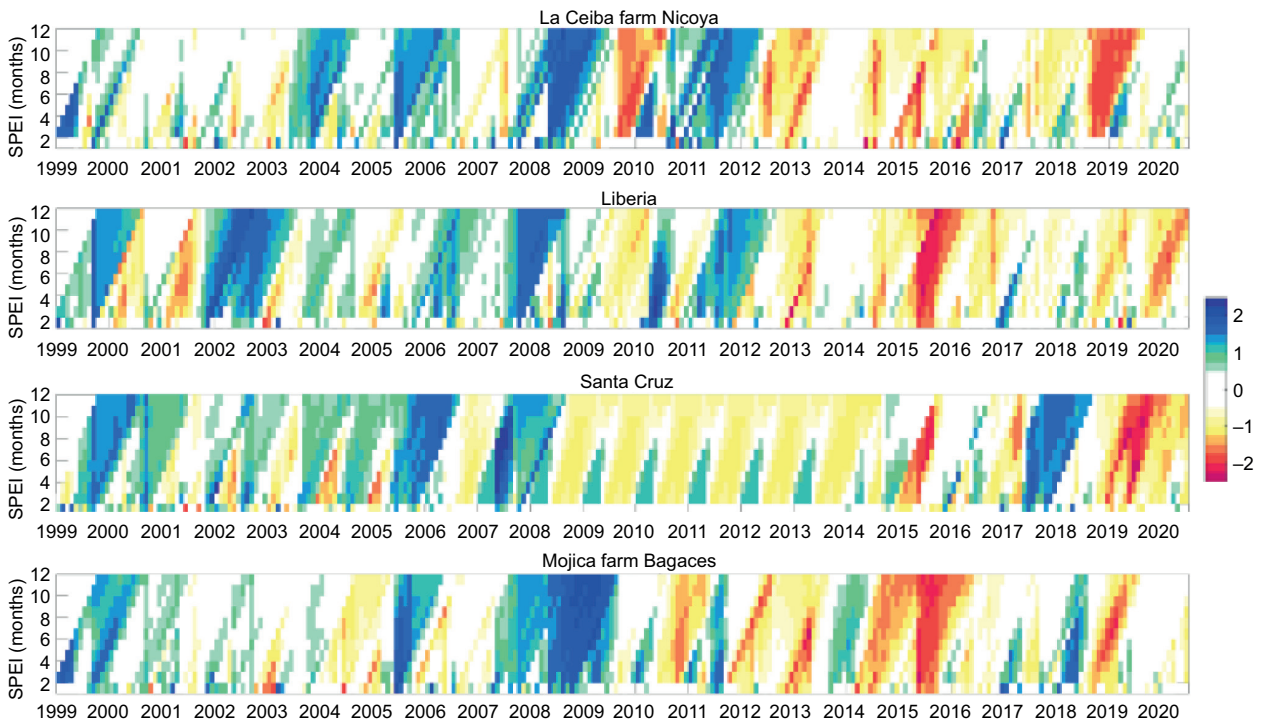


Fig. 4. Occurrence of wet (blue) and dry (red) events, according to SPEI one to 12 months for the stations (a) La Ceiba farm, Nicoya; (b) Liberia, airport; (c) Santa Cruz, and (d) Mojica farm, Bagaces. It is recognized that the second half of the period presents events of greater magnitude and duration in all seasons.

(Fig. 4b). Negative SPEI values were characteristic for Santa Cruz between 2009 and 2014 (Fig. 4c). For Bagaces, the longest drought was identified for the period 2012-2013 (Fig. 4d). The major impact in terms of average deficit was observed during October for Nicoya (-29.76 mm), Liberia (-146.41 mm), Santa Cruz (-148.14 mm), and during September for Bagaces (-98.39 mm), which correspond to the end of the rainy season and are largely influenced by large-scale and synoptic systems that dominate rainfall during the second leg of the rainy season. It is worth mentioning that Santa Cruz also exhibits an important average rainfall deficit during May (-127.67 mm). The results suggest that changes in the large-scale circulation that affect the development of synoptic systems are the main forcing of drought intensification affecting the analysis region during the last decade.

3.3 Influence of ENSO

The ENSO warm phase is associated with warming of the equatorial Pacific waters and changes in the

atmospheric pressure which result in variations of the global circulation patterns. The link between ENSO and drought corresponds to the hydrological response and soil moisture conditions (Vicente-Serrano et al., 2010). It is difficult to accurately establish the impact of ENSO on different types of droughts given the delayed response of vegetation and groundwater systems to the reduction of precipitation and the scarcity of vegetation and depth soil moisture at the local scale. In Central America, warm ENSO is associated with a reduction in precipitation on the Pacific slope (Bonilla, 2014), and the Chorotega region is known for drought development linked to the ENSO warm phase (Cooley et al., 2018). In Costa Rica, prolonged drier periods during warm ENSO have significant impacts on agriculture and forestry, with 90% of drought impacts prior to 1997 directly associated with warm ENSO (Villalobos et al., 1997). According to the historical observational record, ASO (August, September, and October) are the months in which the impact of ENSO is stronger, with significant negative correlations between

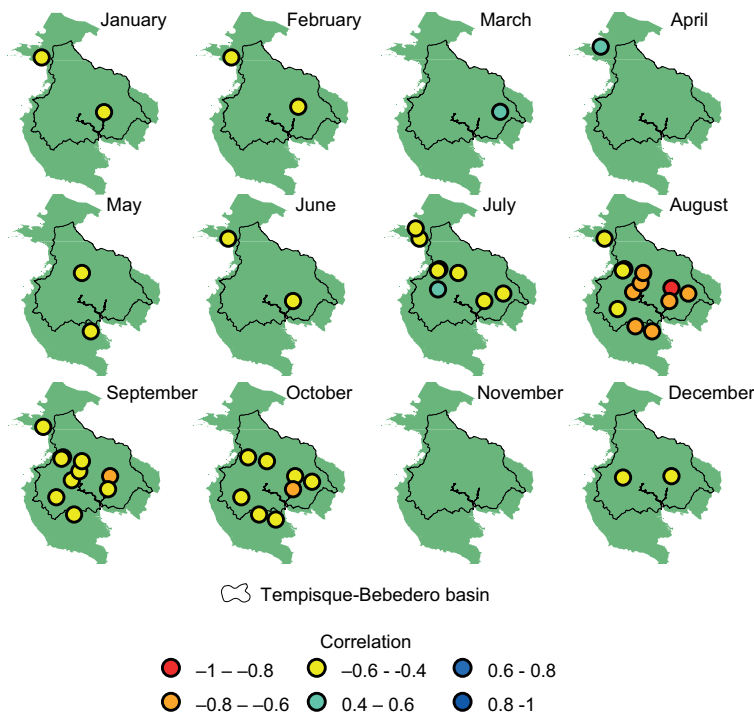


Fig. 5. Monthly (Spearman) correlation between standardized precipitation anomalies and the ENSO Multivariate Index (MEI) for the selected station. All the correlations obtained are of low or moderate significance, except for the correlation in August at Mojica farm, Bagaces. Most of the correlations are negative, except for March, April, and July. The results show that the main impact of ENSO on rainfall occurs during the second leg of the rainy season, the period in which rainfall is dominated by synoptic and large-scale systems. Only significant correlations at the 95% confidence level are shown.

precipitation anomalies and MEI (Fig. 5). Significant ($p < 0.05$) negative correlations are identified for the rainiest months in the Tempisque and Nicoya areas, while less significant correlations are identified for the northwestern area of the Chorotega region.

4. Drought under warming scenarios

Different modeling outputs are available to evaluate future precipitation and temperature conditions based on warming scenarios, most of them corresponding to the Coupled Model Intercomparison Projects (CMIP5, CMIP6) and others that consider the representative concentration pathways (RCPs) under different concentrations of emissions, as well as land use and cover (Moss et al., 2010) or the Shared Socioeconomic Pathways (SSPs) (O'Neill et al., 2014). To assess the projected behavior of drought under warming scenarios, the direct use of climate scenarios generated with global circulation models (GCMs) was discarded given the spatial heterogeneity of agricultural drought identified using observations as shown in section 3. For small regions with complex surfaces, the evaluation of drought requires a better representation of surface processes and surface-atmosphere feedbacks, hence

the use of GCMs products alone is not advised as they may fail to properly reproduce surface conditions, limiting the capacity of estimations to identify drought occurrence and propagation features at regional and local scales. Furthermore, the fragmented landscape and changing land use and vegetation coverage is another limitation for both GCMs and hydrostatic RCMs, as their native resolution may not account for such changes, thus neglecting the role of surface dynamics for drought development. To evaluate the projected behavior of drought events, regional climate projections generated using oceanic coupled future climate scenarios were used as described in section 2. A direct comparison between the observed and modeled monthly mean temperature and accumulated precipitation was conducted for the historical period as a first approximation of the model capacity to reproduce the analysis region's long-term climate conditions. Average standard deviations for the modeled and observed time series for mean temperature and accumulated precipitation are reported as 0.64 °C and 31.22 mm, respectively. We acknowledge the importance of estimating the uncertainty and propagation of errors, however those estimations are beyond the scope of this work. Ocean coupled projections based

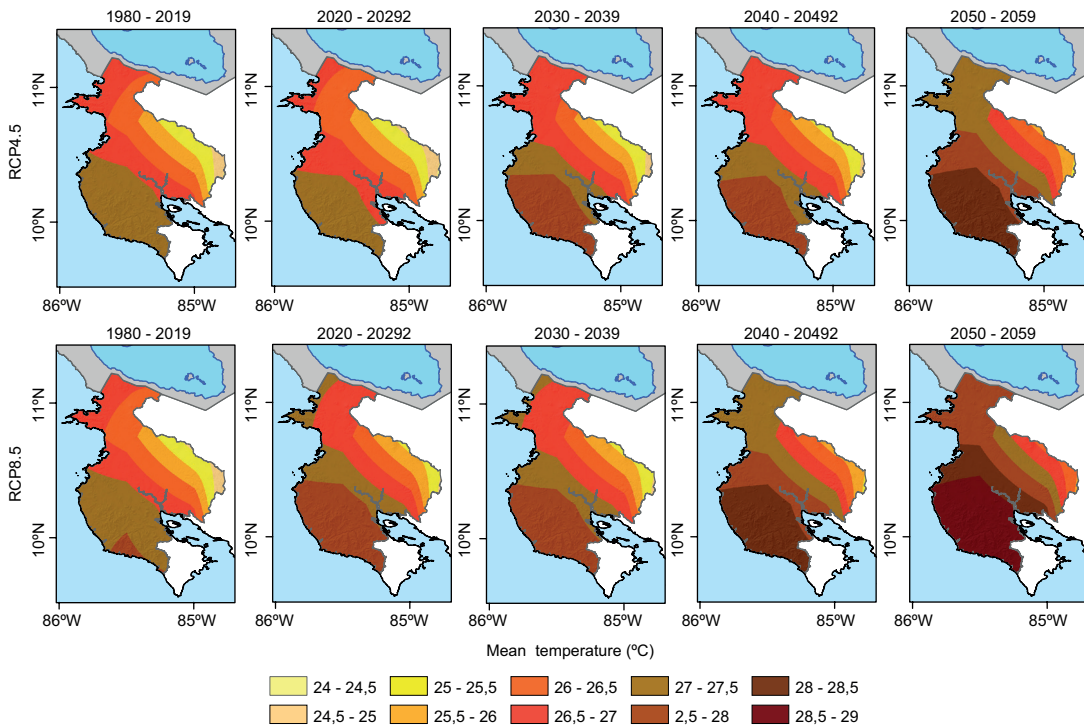


Fig. 6. Projected patterns of average annual temperature according to RCP4.5 (top) and RCP8.5 (bottom) for the historical period (1980-2019) and variations at decadal scale until 2059. The most important increases in temperature are projected to occur over the southern coastal sector and the Nicoya Peninsula.

on RCP4.5 show, in general, a smaller increase in mean temperature for the region after 2050 compared to RCP8.5 scenarios, for which the projected increase surpasses 1 °C after 2040 (Fig. 6).

For agricultural areas, the case of variations in temperature extremes is important, both for the crop's development as well as for the thermal comfort and health of farm workers. Based on the results, the maximum temperature is projected to increase with the warmest conditions projected over the Tempisque-Bebedero catchment area under both RCPs (not shown).

Under RCP4.5 and RCP8.5, precipitation is projected to be reduced over the region (Fig. 7) with nearly half of the precipitation projected to decrease under extreme conditions given by RCP8.5. The identified reduction of precipitation, based on the projections, suggests the Tempisque-Bebedero catchment to be the most affected area. The latter is relevant considering the volume of agricultural activity developed in this region and also the location of the so-called irrigation district. Projections of the

coupled simulations based on RCP4.5 suggest that severe impacts in terms of precipitation decrease would be expected in the next 30 years with an average reduction of 400-800 mm in annual precipitation in the next two decades. Such conditions represent a threat to water availability and severely compromise food security.

Projected decreases (increases) in precipitation (temperature) for both scenarios will likely translate into potential conditions to favor the development of severe drought, particularly after 2050. RCP4.5-based projections suggest a higher relative variability for meteorological drought as estimated for projected SPI-12 (not shown) with severely dry conditions but still possibilities of wet events in between. While a similar behavior is projected for the region, there may be spatial differences related to the length of the drought events. According to projections based on RCP8.5, the dry conditions would be more extreme, with less variability and the possibility for more near-permanent dry conditions towards the end of the century. It is important to mention that projec-

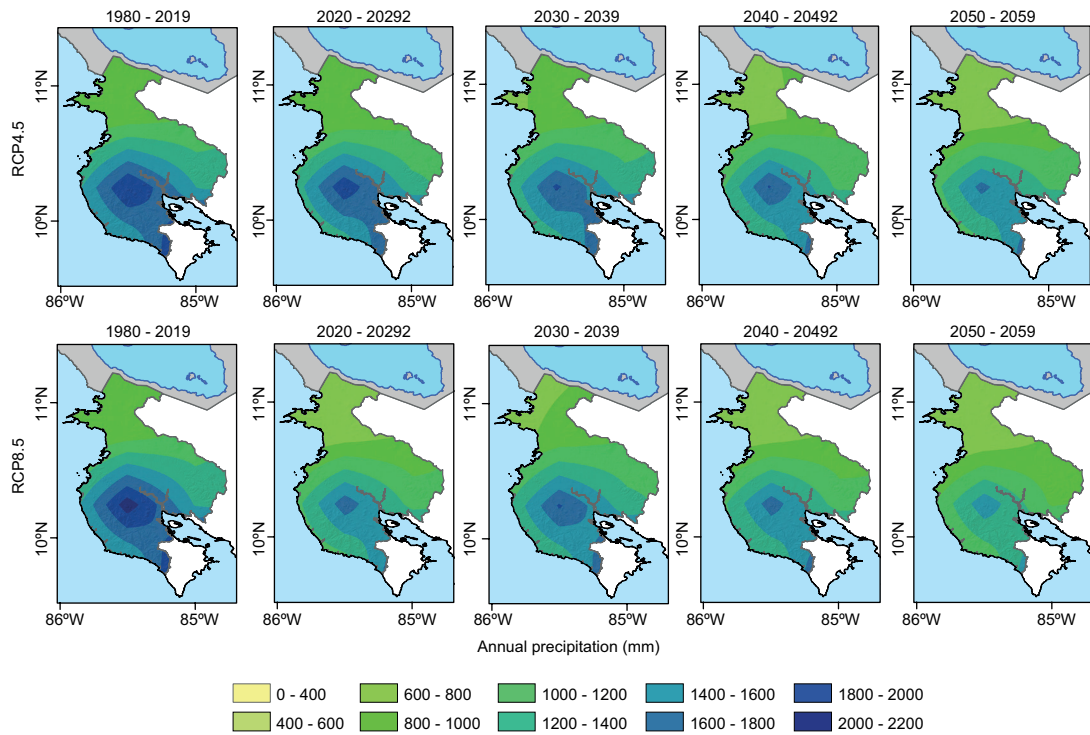


Fig. 7. Projected rainfall based on RCP4.5 (top) and RCP8.5 (bottom) for the historical period (1980-2019) and the following decades until 2059. The most intense drying in the region is projected for the Tempisque-Bebedero basin.

tions to the end of the century should be carefully analyzed as the bias in the simulations increases for longer periods. The case for agricultural drought is similar as estimated from Hargreaves-based SPEI-12 (Fig. 8) with variations in terms of the intensity of the drought events. In general terms, the projections suggest an increase in the drought frequency and severity with consequent impacts on the ecological and productive sectors.

5. Discussion

5.1 Deficit precipitation influence and ET estimates in the drought evaluation

Analysis of extreme precipitation is known to be hindered by the availability of observational records. Albeit the identification of meteorological drought can be conducted based on available precipitation data, the assessment of agricultural drought relies on the capacity to estimate ET as the main component of the water balance and key in the surface-atmosphere coupling, which defines the transport of water fluxes.

The use of the Hargreaves method provides a relatively uniform ET throughout the year as it is biased by the weight of the extraterrestrial radiation input in the estimation of ET.

Because the SPI only considers changes in precipitation (Vicente-Serrano et al., 2014), local variations in surface fluxes relevant to determine the surface-atmosphere feedback that modulates the atmospheric are not accounted and the assessment of meteorological drought is likely underestimated for the Chorotega region. In this regard, the use of SPI alone may not be suitable to support decision-making beyond the identification of precipitation deficits and may not be representative of the spatial variability of meteorological drought in the region. Furthermore, the normal distribution of rainfall data considered in the estimation of SPI conducts to a similar register in the frequency of dry events for a region as shown by Hayes et al. (1999). For small areas in which rainfall presents a heterogeneous spatial distribution and marked dry season as is the case for the Chorotega region, the drought assessment

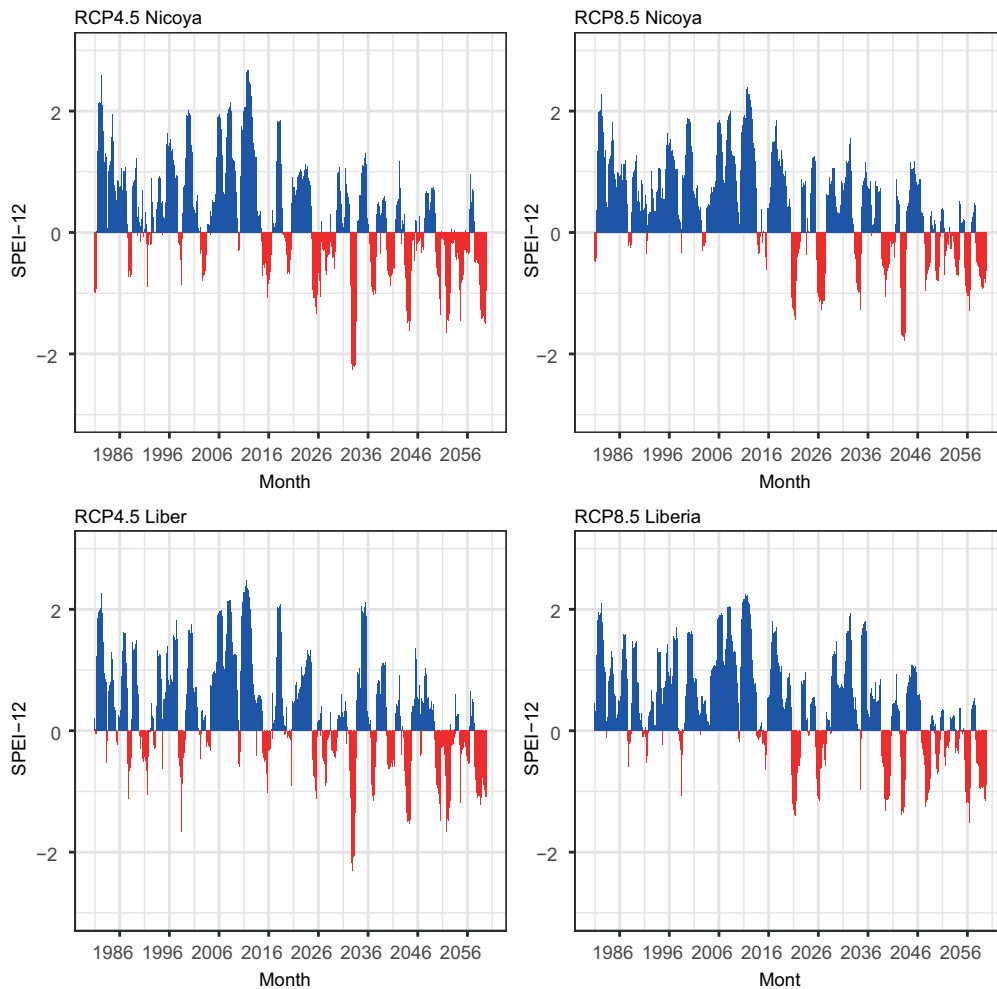


Fig. 8. SPEI-12 projected values for Nicoya (top) and Liberia (bottom) according to the RCP4.5 (left) and RCP8.5 (right) scenarios. Similar behavior of variability in the hydrological drought conditions between the two stations is presented under the RCP4.5 scenario. In the RCP8.5 scenario, there are differences between stations and dry conditions become more severe.

must be carefully carried out because the method fails to properly capture low SPI values under conditions with a high probability of day without rainfall as suggested by Wu et al (2007). In contrast, the identification of meteorological drought using SPEI accounts for the atmospheric demand and it is not limited by the soil moisture content or available rainfall (Vicente-Serrano et al., 2014). In areas with low rainfall, the estimation method plays a main role in the water balance and SPEI becomes dependent on the rainfall reduction, while in wetter areas SPEI is more dependent on the magnitude of the decrease in ET_0 (Begueria et al., 2014). As a general result of this evaluation, the identification of drought events

is biased depending on the implemented method, and to better inform drought risk, evolution, and impacts, the use of methods that better account for ET is recommended.

5.2 Impact of ENSO over observed drought events in northwestern Costa Rica

Previous studies show the ENSO warm phase to be associated with drought development in northwestern Costa Rica. However, the spatial variability of drought events occurrence and severity in the region is understudied. The impact of warm ENSO on the reduction of precipitation is larger during the second leg of the rainy season, a period in which precipitation

is mostly forced by large and synoptic-scale systems. Warm ENSO reduces the potential for tropical storms and cyclones to develop in the tropical Atlantic and Caribbean and causes a displacement of the convergence zone to the eastern tropical Pacific, causing an overall reduction of rainfall in the Chorotega region. During the second leg of the rainy season, rainfall in the study area is generated by the systems that are suppressed under warm ENSO, largely affecting the rainfall input for the Tempisque-Bebedero area, a region of extensive agricultural activities. Based on the observations, Tempisque-Bebedero is affected by more agricultural drought events in contrast with fewer agricultural droughts affecting the Nicoya Peninsula, for which forested areas are preserved, in the same period. The vegetation coverage, jointly with the soil type, can act as a buffer for the propagation of drought conditions across the components of the hydrological cycle. In this sense, extensive mono-crops are common in the areas that were found to be more affected by the propagation of the drought in the Chorotega region. Regardless agricultural droughts exhibit spatial heterogeneity, they have become more severe in the recent decades for all analyzed sites, as shown by larger negative SPEI values in Figure 4. Moreover, the results show that agricultural drought events are becoming more intense, and at the same time their occurrence is more prolonged as warm ENSO events have increased their occurrence and intensity. Although this study did not consider the impact irrigation may have, it was mentioned that irrigation may play a role in the lack of response of NDVI to drought propagation. The fact that most agricultural drought events were identified in areas with extensive farming may imply more irrigation is required to maintain the crops, causing further impacts on the availability of water for the communities and contributing to the overexploitation of groundwater resources. Hence, mitigation measures can be proposed for the agricultural lands in the Tempisque-Bebedero basin such as improving permanent vegetation coverage to buffer the propagation of the meteorological to agricultural drought.

5.3. Projected drought events under warming scenarios

Both RCP 4.5 and RCP 8.5 project temperature to increase in the Chorotega region and the reduction

of total annual rainfall by mid-century, with changes being more severe under RCP 8.5. Projected warming and drying present a marked spatial variability, with variations being more exacerbated over the Nicoya Peninsula and the Tempisque-Bebedero basin. For those locations, warming scenarios suggest the likely development of severe drought. Drought events are projected to be severe and propagate across the hydrological system because of the combination of large-scale and local conditions. On one hand, warming results in the displacement of the convergence cells and changes in the synoptic systems that generate rainfall in the Chorotega region while the increase in surface temperature contributes to the increase in the evaporative demand of the atmosphere. This means that changes in the large and synoptic scale systems drive the occurrence of the meteorological drought and the local warming enhances the propagation of the agricultural drought. Such aggravation of drought events in the region is consistent with studies showing that the signal of drought in the region consists of the combined effect of warm ENSO and climate change (Pascale et al., 2021). Albeit we acknowledge projected drought results are biased by the resolution of the coupled regional simulations and the limitations of the statistical downscaling, the method implemented allows to identify variations in the projected drought in the local scale which are consistent with observations for the historical period. Even when the assessment of observed impacts of climate variability and change on the behavior of drought in the southern portion of the CADC is hindered by the lack of long-term quality observations, a robust regional climate modeling approach can provide reliable information to assess past and future variations of dry extremes. In the case of the Chorotega region, the projected intensification of agricultural drought events highlights the need to develop integral planning that can guarantee access to water resources and the need to enforce sustainability of agricultural and tourism activities to reduce the impact of land use and vegetation changes on local warming and promote the restoration of the soil to reduce the risk of desiccation. It is important to consider that the use of climate scenarios derived from RCM simulations is still biased in terms of the resolution, which means that mechanisms related to the propagation of drought that are directly related

to surface feedback processes are underrepresented given the resolution limit of the hydrostatic models. Further development of observational datasets for validation and integration of soil moisture and temperature is advised to include bias correction methods that can improve the spatial quality of the simulations to better represent the system.

6. Conclusions

This study contributes to the assessment of historical drought in the southern portion of the CADC and the evaluation of the projected behavior of drought in the region based on regional dynamically down-scaled ocean-coupled climate projections. The study focuses on the relevance of identifying the type of drought to better identify risk areas and inform water resources management stakeholders. Despite the scarcity of high-quality long-term historical records, available information enables the identification of spatial variability in the development of agricultural drought. The detection of trends in drought frequency and intensity that may be attributed to observed climate change was not possible given the length of the records. The main results show:

- Consistent warming trends are a proxy for a significant increase in atmospheric demand, suggesting an impact of warming in the feedback mechanism for drought auto-intensification in the Chorotega region. However, the quantification of the impact of warming on soil desiccation and the correspondent influence on the propagation of drought was not possible at this stage given the lack of soil moisture observations and the rather poor performance of soil moisture satellite estimates.
- The spatial variability of ET shows the atmospheric demand is larger in the northernmost portion of the Chorotega region, which results in differences in terms of drought forcing as a larger fraction of rainfall becomes a water flux back to the atmosphere. The latter contributes to the enhancement of the water deficit in the region and increases the pressure on the water resources in the irrigation district compared to other locations. This is a relevant aspect to be considered in terms of water resources planning as the severity of the events has a well-defined spatial variability.
- The impact of El Niño is more significant during the second leg of the rainy season, because the teleconnection pattern affects the development of synoptic systems and their interaction with the Inter-Tropical Convergence Zone, reducing the amount of rainfall in the region. This causes a limitation in the surface moisture availability which can prolong the dry season and enhance the propagation of drought across the hydrological cycle compartments, exacerbating the problem of water resources availability and the pollution of aquifers. Sustainable land use and vegetation coverage management can alleviate this impact by contributing to the reduction of surface water loss, and planning of irrigation and water for human consumption must follow the ENSO warning advisories. Further development of early warning capacities requires the strengthening of seasonal forecasts.
- Ocean-coupled regional climate projections show consistency in increasing temperatures, with the Nicoya Peninsula experiencing the largest temperature increase, while a generalized rainfall decrease is projected for the Chorotega region, with Tempisque-Bebedero basin and the Nicoya Peninsula projected to experience the most significant precipitation reduction. The identification of drought severity under warming scenarios is still biased by the native resolution of the model, suggesting that complementary information must be included in these types of studies, particularly the coupling of the RCMs results with hydrological models.
- Future climate scenarios draw attention to the potential decrease in rainfall and likely intensification of dry conditions towards the end of the century, posing a major threat to the rain-fed agricultural activities developed in the irrigation district area. The development of a soil moisture monitoring network will provide a better estimate of the propagation of drought across the system and enable access to improved modeling validation frameworks to advance drought assessment and forecasting.

The attribution of climate variability and change impact on drought development is still challenging. The scarcity of data to provide a robust assessment of ET is one of the main constraints. The skill of global climate models to reproduce surface processes is often highlighted as a challenge in the study of small regions, with dynamic downscaling intended to fill in the gap between global and regional scales (Tapiador et al., 2020). Data and modeling integration are needed to advance the comprehension of the dynamics between the response of vegetation and the atmospheric demand during the development and propagation of drought. The representation of vegetation dynamics within regional climate models persists as a main constraint in the representation of model-based surface energy fluxes and ET. The accuracy of climate scenarios to adequately inform precipitation and temperature likely changes is still dependent on the improvement of spatial resolution, given the spatial variability of observed events at relatively small scales. With the increasing demand for projected climate products for planning, as well as decision and policy making, the advancement of current modeling capacity must be accompanied by significant upgrades of the monitoring systems.

Acknowledgments

The development of this work was funded by the MICITT grant (project UCR-B9519) and observational records were provided by the Costa Rica National Meteorological Institute under agreement DIM-CM-117-0917. AMDQ was funded by IAEA F31006 and UCR grant C1038. HH is funded by the following projects from the University of Costa Rica: B9-454 (VI-Grupos), EC-497 (FEES-CONARE), C0-610 (Fondo de Estímulo), A4-906 (PESCT-MA-CIGEFI), C0-074, A1-715, B0-810 and A5-037. CB would like to acknowledge UCR support for the Water and Global Change (OACG) Observatory (C2902) and the DAAD funded TropiSeca project. DVS was supported by the Germany-Sino Joint Project (ACE, No. 2019YFE0125000 and 01LP2004A) and MHESRF scientific task No FMWE-2024-0028.

References

Alfaro EJ. 2014. Caracterización del “veranillo” en dos cuencas de la vertiente del Pacífico de Costa Rica,

América Central (Characterization of the mid-summer drought in two Pacific slope river basin of Costa Rica, Central America). *International Journal of Tropical Biology* 62: 1-15. <https://doi.org/10.15517/rbt.v62i4.20010>

Alfaro-Córdoba M, Hidalgo HG, Alfaro EJ. 2020. Aridity trends in Central America: A spatial correlation analysis. *Atmosphere* 11: 427. <https://doi.org/10.3390/atmos11040427>

Amador JA, Rivera ER, Durán-Quesada AM, Mora G, Sáenz F, Calderón B, Mora N. 2016. The easternmost tropical Pacific. Part I: A climate review. *Revista de Biología Tropical* 64: S1-S22. <https://doi.org/10.15517/rbt.v64i1.23407>

Anderegg W.R, Trugman A.T, Badgley G, Konings A.G, Shaw J. 2020. Divergent forest sensitivity to repeated extreme droughts. *Nature Climate Change* 10: 1091-1095. <https://doi.org/10.1038/s41558-020-00919-1>

Bador M, Boé J, Terray L, Alexander LV, Baker A, Bellucci A, Haarsma R, Koenigk T, Moine M.P, Lohmann K, Putrasahan D, Roberts C, Roberts M, Scoccimarro E, Schiemann R, Seddon J, Senan R, Valcke S, Vanniere, B. (2020). Impact of higher spatial atmospheric resolution on precipitation extremes over land in global climate models. *Journal of Geophysical Research: Atmospheres* 125: e2019JD032184. <https://doi.org/10.1029/2019JD032184>

Bacon CM, Sundstrom WA, Stewart IT, Beezer D. 2017. Vulnerability to cumulative hazards: Coping with the coffee leaf rust outbreak, drought, and food insecurity in Nicaragua. *World Development* 93: 136-152. <https://doi.org/10.1016/j.worlddev.2016.12.025>

Beguiría S, Vicente-Serrano SM, Reig F, Latorre B. 2014. Standardized precipitation evapotranspiration index (SPEI) revisited: Parameter fitting, evapotranspiration models, tools, datasets and drought monitoring. *International Journal of Climatology* 34: 3001-3023. <https://doi.org/10.1002/joc.3887>

Birkel C, Demuth S. 2006. Drought in Costa Rica: Temporal and spatial behaviour, trends and the relationship to atmospheric circulation patterns. *International Conference on FRIEND*. Havana, Cuba, November. IAHS Red Book, 338- 343.

Bonilla A. 2014. Patrones de sequía en Centroamérica. Su impacto en la producción de maíz y frijol y uso del Índice Normalizado de Precipitación para los sistemas de alerta temprana. *Global Water Partnership*, Tegucigalpa, Honduras.

- Cabos W, Sein DV, Durán-Quesada A, Liguori G, Koldunov NV, Martínez-López B, Álvarez F, Sieck K, Limareva N, Pinto JG. 2019. Dynamical downscaling of historical climate over CORDEX Central America domain with a regionally coupled atmosphere-ocean model. *Climate Dynamics* 52: 4305-4328. <https://doi.org/10.1007/s00382-018-4381-2>
- Campos-Vargas C, Vargas-Sanabria D. 2021. Assessing the probability of wildfire occurrences in a neotropical dry forest. *Écoscience* 28: 159-169. <https://doi.org/10.1080/11956860.2021.1916213>
- Casanova OP. 1993. Riesgo por sequías en Costa Rica. *Revista Geográfica de América Central* 25-26: 385-405.
- Castro SM, Sánchez-Azofeifa GA, Sato H. 2018. Effect of drought on productivity in a Costa Rican tropical dry forest. *Environmental Research Letters* 13: p.045001. <https://doi.org/10.1088/1748-9326/aaacbc>
- Chaware S, Taley SM, Jadhav SU. 2017. Performance of different methods of estimating potential evapotranspiration in western Vidarbha region. *Contemporary Research in India* 7: 417-420.
- Cooley SS, Williams CA, Fisher JB, Halverson GH, Perret J, Lee CM. 2018. Assessing regional drought impacts on vegetation and evapotranspiration: A case study in Guanacaste, Costa Rica. *Ecological Applications* 29: e01834. <https://doi.org/10.1002/eap.1834>
- Coto Hernández M. 2016. Paacume: más que un proyecto de infraestructura, un proyecto de desarrollo. *Ambientico* 260: 3-37.
- Diffenbaugh NS, Pal JS, Trapp RJ, Giorgi F. 2005. Fine-scale processes regulate the response of extreme events to global climate change. *Proceedings of the National Academy of Sciences* 102: 15774-15778. <https://doi.org/10.1073/pnas.0506042102>
- Donohue RJ, McVicar TR, Roderick ML. 2010. Assessing the ability of potential evaporation formulations to capture the dynamics in evaporative demand within a changing climate. *Journal of Hydrology* 386: 186-197. <https://doi.org/10.1016/j.jhydrol.2010.03.020>
- Dunn SM, Mackay R. 1995. Spatial variation in evapotranspiration and the influence of land use on catchment hydrology. *Journal of Hydrology* 171: 49-73. [https://doi.org/10.1016/0022-1694\(95\)02733-6](https://doi.org/10.1016/0022-1694(95)02733-6)
- Durán-Quesada AM, Sorí R, Ordóñez P, Gimeno L. 2020. Climate perspectives in the Intra-Americas seas. *Atmosphere* 11: p.959. <https://doi.org/10.3390/atmos11090959>
- Gagnon AS, Smoyer-Tomic KE, Bush AB. 2002. The El Niño Southern Oscillation and malaria epidemics in South America. *International Journal of Biometeorology* 46: 81-89. <https://doi.org/10.1007/s00484-001-0119-6>
- García-Franco JL, Chadwick R, Gray LJ, Osprey S, Adams DK. 2022. Revisiting mechanisms of the Mesamerican midsummer drought. *Climate Dynamics* 60: 549-569. <https://doi.org/10.1007/s00382-022-06338-6>
- González Villareal C, Vilaboa R. 2010. Informe final de investigación: tendencias del desarrollo en el cantón de Santa Cruz, Guanacaste. Período 1979-2009. Universidad Estatal a Distancia, Instituto de Formación y Capacitación Municipal y de Desarrollo Local, Costa Rica. Available at <https://silo.tips/download/resultados-del-estudio-tendencias-del-desarrollo-en-el-canton-de-santa-cruz-guan> (accessed 2020 June 12).
- Green JK, Konings AG, Alemohammad SH, Berry J, Entekhabi D, Kolassa J, Lee JE, Gentine P. 2017. Regionally strong feedback between the atmosphere and terrestrial biosphere. *Nature Geoscience* 10: 410-417. <https://doi.org/10.1038/ngeo2957>
- Hargreaves GH. 1994. Defining and using reference evapotranspiration. *Journal of Irrigation and Drainage Engineering* 120: 1132-1139. [https://doi.org/10.1061/\(ASCE\)0733-9437\(1994\)120:6\(1132\)](https://doi.org/10.1061/(ASCE)0733-9437(1994)120:6(1132))
- Hayes MJ, Svoboda MD, Wilhite DA, Vanyarkho OV. 1999. Monitoring the 1996 drought using the standardized precipitation index. *Bulletin of the American Meteorological Society* 80: 429-438 [https://doi.org/10.1175/1520-0477\(1999\)080<0429:MTDUTS>2.0.CO;2](https://doi.org/10.1175/1520-0477(1999)080<0429:MTDUTS>2.0.CO;2)
- Hernández Contreras JL. n.d. Informe final de labores. Dirección Regional Chorotega. Servicio de Salud Animal, Ministerio de Agricultura y Ganadería, Costa Rica. Available at <https://www.mag.go.cr/transparencia/informes%20de%20fin%20de%20gestion/Inf-JoseLuis-H.pdf> (accessed 2020 August 05).
- Hidalgo HG, Cayan DR, Dettinger MD. 2005. Sources of variability of evapotranspiration in California. *Journal of Hydrometeorology* 6: 3-19. <https://doi.org/10.1175/JHM-398.1>
- Hidalgo HG, Alfaro EJ, Amador JA, Bastidas A. 2019. Precursors of quasi-decadal dry-spell in the Central America dry corridor. *Climate Dynamics* 53: 1307-1322. <https://doi.org/10.1007/s00382-019-04638-y>
- InfoAgro. 2015. Plan Regional de Desarrollo Agropecuario y Rural 2015-2018. Sistema de Información del Sector Agropecuario Costarricense, San José, Costa Rica.
- Jacob D, van den Hurk BJJM, Andrae U, Elgered G, Fortelius C, Graham LP, Jackson SD, Karstens U, Köpen

- C, Lindau R, Podsun R, Rockel B, Rubel F, Sass BH, Smith RNB, Yang, X. 2001. A comprehensive model inter-comparison study investigating the water budget during the BALTEX-PIDCAP period. *Meteorology and Atmospheric Physics* 77: 19-43. <https://doi.org/10.1007/s007030170015>
- Ji L, Peters AJ. 2003. Assessing vegetation response to drought in the northern Great Plains using vegetation and drought indices. *Remote Sensing of Environmental* 87: 85-98. [https://doi.org/10.1016/S0034-4257\(03\)00174-3](https://doi.org/10.1016/S0034-4257(03)00174-3)
- Jiménez JC, Marengo JA, Alves LM, Sulca JC, Takahashi K, Ferrett S, Collins M. 2021. The role of ENSO flavours and TNA on recent droughts over Amazon forests and the Northeast Brazil region. *International Journal of Climatology* 41: 3761-3780. <https://doi.org/10.1002/joc.6453>
- Koster RD, Dirmeyer PA, Guo Z, Bonan G, Chan E, Cox P, Gordon C.T, Kanae S, Kowalczyk E, Lawrence D, Liu P, Lu CH, Malyshev S, McAvaney B, Mitchell K, Mocko D, Oki T, Oleson K, Pitman A, Sud YC, Taylor CM, Verseghy D, Vasic R, Xue Y, Yamada T. 2004. Regions of strong coupling between soil moisture and precipitation. *Science* 305: 1138-1140. <https://doi.org/10.1126/science.1100217>
- Lemordant L, Gentine P. 2019. Vegetation response to rising CO₂ impacts extreme temperatures. *Geophysical Research Letters* 46: 1383-1392. <https://doi.org/10.1029/2018GL080238>
- Liu Y, Zhuang Q, Pan Z, Miralles D, Tchebakova N, Kicklighter D, Chen J, Sirin A, He Y, Zhou G, Mellillo J. 2014. Response of evapotranspiration and water availability to the changing climate in Northern Eurasia. *Climatic Change* 126: 413-427. <https://doi.org/10.1007/s10584-014-1234-9>
- Logar I, van den Bergh JC. 2013. Methods to assess costs of drought damages and policies for drought mitigation and adaptation: review and recommendations. *Water Resources Management* 27: 1707-1720. <https://doi.org/10.1007/s11269-012-0119-9>
- López-Moreno JI, Vicente-Serrano SM, Beguería S, García-Ruiz JM, Portela MM, Almeida AB. 2009. Dam effects on droughts magnitude and duration in a transboundary basin: The lower river Tagus, Spain and Portugal. *Water Resources Research* 45: W02405. <https://doi.org/10.1029/2008WR007198>
- Machado-Silva F, Libonati R, de Lima TFM, Peixoto RB, de Almeida Franca JR, Magalhães MDAFM, Santos FLM, Rodrigues JA, DaCamara CC. 2020. Drought and fires influence the respiratory diseases hospitalizations in the Amazon. *Ecological Indicators* 109: p.105817. <https://doi.org/10.1016/j.ecolind.2019.105817>
- Magaña V, Amador JA, Medina S. 1999. The midsummer drought over Mexico and Central America. *American Meteorological Society* 12: 1577-1588. <https://doi.org/10.1002/joc.6296>
- Maidment D.R. 1993. *Handbook of hydrology*. McGraw-Hill.
- Maldonado T, Rutgersson A, Alfaro E, Amador J, Claremar B. 2016. Interannual variability of the midsummer drought in Central America and the connection with sea surface temperatures. *Advances in Geosciences* 42: 35-50. <https://doi.org/10.5194/adgeo-42-35-2016>
- Marsland SJ, Haak H, Jungclaus JH, Latif M, Roeske F. 2002. The Max-Planck-Institute global ocean/sea ice model with orthogonal curvilinear coordinates. *Ocean Modell* 5: 91-126. [https://doi.org/10.1016/S1463-5003\(02\)00015-X](https://doi.org/10.1016/S1463-5003(02)00015-X)
- Martens B, Waegeman W, Dorigo WA, Verhoest NE, Miralles DG. 2018. Terrestrial evaporation response to modes of climate variability. *NPJ Climate and Atmospheric Science* 1: 43. <https://doi.org/10.1038/s41612-018-0053-5>
- Maurer EP, Stewart IT, Joseph K, Hidalgo HG. 2022. The Mesoamerican mid-summer drought: the impact of its definition on occurrences and recent changes. *Hydrology and Earth System Sciences* 26: 1425-1437. <https://doi.org/10.5194/hess-26-1425-2022>
- McCabe MF, Miralles DG, Holmes TR, Fisher JB. 2019. Advances in the remote sensing of terrestrial evaporation. *Remote Sensing* 11: 1138. <https://doi.org/10.3390/rs11091138>
- McKee T B, Doesken NJ, Kleist J. 1993. The relationship of drought frequency and duration to time scales. In: *Proceedings of the 8th Conference on Applied Climatology*, 179-184. Anaheim, January 17-22, 179-184.
- Meneses-Tovar CL. 2011. El índice normalizado diferencial de vegetación como indicador de la degradación del bosque. *Unasyuva* 238: 39-45.
- Meza I, Siebert S, Döll P, Kusche J, Herbert C, Eyshi Rezaei E, Nouri H, Gerdener H, Popat E, Frischen J, Naumann G. 2020. Global-scale drought risk assessment for agricultural systems. *Natural Hazards and Earth System Sciences* 20: 695-712. <https://doi.org/10.5194/nhess-20-695-2020>

- Miralles D, Gentile P, Seneviratne SI, Teuling AJ. 2019. Land-atmospheric feedbacks during droughts and heatwaves: State of the science and current challenges. *Annals of the New York Academy of Sciences* 1436: 19-35. <https://doi.org/10.1111/nyas.13912>
- Monteith JL. 1965. Evaporation and environment, in the state and movement of water in living organisms. *Proceedings of the Society for Experimental Biology, Symposium No. 19*, Cambridge University Press, Cambridge, 1965, 205-234.
- Mora Alvarado D, Portuguez CF. 2012. Calidad del agua en sus diferentes usos en Guanacaste – Costa Rica al año 2011. Instituto Costarricense de Acueductos y Alcantarillados, San José, Costa Rica.
- Moss R, Edmonds J, Hibbard K, Manning M, Rose S, van Vuuren D, Carter T, Emori S, Kainuma M, Kram T, Meehl G, Mitchell J, Nakicenovic N, Riahi K, Smith S, Stouffer R, Thomson A, Weyant J, Wilbanks T. 2010. The next generation of scenarios for climate change research and assessment. *Nature* 463: 747-756. <https://doi.org/10.1038/nature08823>
- Mukherjee S, Mishra A, Trenberth KE. 2018. Climate change and drought: A perspective on drought indices. *Current Climate Change Reports* 4: 145-163. <https://doi.org/10.1007/s40641-018-0098-x>
- Mullin M. 2020. The effects of drinking water service fragmentation on drought-related water security. *Science* 368: 274-277. <https://doi.org/10.1126/science.aba7353>
- O'Neill BC, Krieglner E, Riahi K, Ebi KL, Hallegatte S, Carter TR, Mathur R, van Vuuren DP. 2014. A new scenario framework for climate change research: The concept of shared socioeconomic pathways. *Climatic change* 122: 387-400. <https://doi.org/10.1007/s10584-013-0905-2>
- Özger M, Mishra AK, Singh VP. 2009. Low-frequency drought variability associated with climate indices. *Journal of Hydrology* 364: 152-162. <https://doi.org/10.1016/j.jhydrol.2008.10.018>
- Pascale S, Kapnick SB, Delworth TL, Hidalgo HG, Cooke WF. 2021. Natural variability vs. forced signal in the 2015-2019 Central American drought. *Climatic Change* 168: 1-21. <https://doi.org/10.1007/s10584-021-03228-4>
- Ramírez P. 1983. Estudio meteorológico de los veranillos en Costa Rica. Nota de investigación 5. Ministerio de Agricultura y Ganadería, Costa Rica. Available at <https://www.imn.ac.cr/documents/10179/20909/Estudio+sobre+veranillos+en+Costa+Rica> (accessed 2020 June 20)
- Ramírez Villegas G, Jiménez García J. 1998. Diagnóstico general de la situación actual de los recursos hídricos en la provincia de Guanacaste. Guanacaste – Costa Rica. Instituto Costarricense de Acueductos y Alcantarillados, San José, Costa Rica.
- Rind D, Goldberg R, Hansen J, Rosenzweig C, Ruedy R. 1990. Potential evapotranspiration and the likelihood of future drought. *Journal of Geophysical Research: Atmospheres* 95: 9983-10004. <https://doi.org/10.1029/JD095iD07p09983>
- Rozario PF, Madurapperuma BD, Wang Y. 2018. Remote sensing approach to detect burn severity risk zones in Palo Verde National Park, Costa Rica. *Remote Sensing* 10: 1427. <https://doi.org/10.3390/rs10091427>
- Schwalm CR, Anderegg WR, Michalak AM, Fisher J.B, Biondi F, Koch G, Litvak M, Ogle K, Shaw JD, Wolf A, Huntzinger DN. 2017. Global patterns of drought recovery. *Nature* 548: 202-205. <https://doi.org/10.1038/nature23021>
- Sein DV, Mikolajewicz U, Gröger M, Fast I, Cabos W, Pinto JG, Hagemann S, Semmler T, Izquierdo A, Jacob D. 2015. Regionally coupled atmosphere-ocean-sea ice-marine biogeochemistry model ROM: 1. Description and validation. *Journal of Advances in Modeling Earth Systems* 7: 268-304. <https://doi.org/10.1002/2014MS000357>
- Semeraro T, Luvisi A, Lillo AO, Aretano R, Buccolieri R, Marwan N. 2020. Recurrence analysis of vegetation indices for highlighting the ecosystem response to drought events: An application to the Amazon forest. *Remote Sensing* 12: 907. <https://doi.org/10.3390/rs12060907>
- Stahle DW, Cook ER, Burnette DJ, Villanueva J, Cerano J, Burns JN, Griffin D, Cook BI, Acuna R, Torbenson MC, Szejner P. 2016. The Mexican drought atlas: Tree-ring reconstructions of the soil moisture balance during the late pre-Hispanic, colonial, and modern eras. *Quaternary Science Reviews* 149: 34-60. <https://doi.org/10.1016/j.quascirev.2016.06.018>
- Tapiador FJ, Navarro A, Moreno R, Sánchez JL, García-Ortega E. 2020. Regional climate models: 30 years of dynamical downscaling. *Atmospheric Research* 235: 104785. <https://doi.org/10.1016/j.atmosres.2019.104785>
- Taufik M, Torfs PJ, Uijlenhoet R, Jones PD, Murdiyarso D, Van Lanen HA. 2017. Amplification of wildfire area burnt by hydrological drought in the humid

- tropics. *Nature Climate Change* 7: 428-431. <https://doi.org/10.1038/nclimate3280>
- Thackeray CW, Hall A, Norris J, Chen D. 2022. Constraining the increased frequency of global precipitation extremes under warming. *Nature Climate Change* 12: 441-448. <https://doi.org/10.1038/s41558-022-01329-1>
- Valcke S. 2013. The OASIS3 coupler: A European climate modelling community software. *Geoscientific Model Development* 6: 373-388. <https://doi.org/10.5194/gmd-6-373-2013>
- Van der Zee Arias A, Meyrat A, Picado L, Poveda C, van der Zee J. 2012. Estudio de caracterización del corredor seco centroamericano, Organización de las Naciones Unidas para la Alimentación y la Agricultura. Ideas litográficas, Honduras. Available at <http://humanright2water.org/fr/wp-content/uploads/2020/03/1212-Corredor-Seco-Centroamericano.pdf> (accessed 2020 June 10)
- Van Loon AF, van Lanen HAJ. 2012. A process-based typology of hydrological drought. *Hydrology and Earth System Sciences* 16: 1915-1946. <https://doi.org/10.5194/hess-16-1915-2012>
- Van Loon AF. 2015. Hydrological drought explained. *WIREs Water* 2: 359-392. <https://doi.org/10.1002/wat2.1085>
- Van Loon AF, Laaha G. 2015. Hydrological drought severity explained by climate and catchment characteristics. *Journal of Hydrology* 526: 3-14. <https://doi.org/10.1016/j.jhydrol.2014.10.059>
- Van Loon AF, Stahl K, Di Baldassarre G, Clark J, Rangel-Croft S, Wanders N, Glesson T, Van Dijk AIJM, Tallaksen LM, Hannaford J, Uijlenhoet R, Teuling AJ, Hannah DM, Sheffield J, Svoboda M, Verbeiren B, Wagener T, Van Lanen HAJ. 2016. Drought in a human-modified world: reframing drought definitions, understanding, and analysis approaches. *Hydrological and Earth System Sciences* 20: 3631-3650. <https://doi.org/10.5194/hess-20-3631-2016>
- Vargas G. 2006. Geografía de Costa Rica. EUNED, San José, Costa Rica.
- Vicente-Serrano SM, Beguería S, López-Moreno JI. 2010. A multiscale drought index sensitive to global warming: the standardized precipitation evapotranspiration index. *Journal of Climate* 23: 1696-1718. <https://doi.org/10.1175/2009JCLI2909.1>
- Vicente-Serrano SM, López-Moreno JI, Gimeno L, Nieto R, Morán-Tejeda E, Lorenzo-Lacruz J, Beguería S, Azorín-Molina C. 2011. A multiscale global evaluation of the impact of ENSO on droughts. *Journal of Geophysical Research Atmospheres* 116: D20109. <https://doi.org/10.1029/2011JD016039>
- Vicente-Serrano SM, Schrier Gvd, Beguería S, Azorín-Molina C, López-Moreno J-I. 2014. Contribution of precipitation and reference evapotranspiration to drought indices under different climates. *Journal of Hydrology* 526: 42-54. <https://doi.org/10.1016/j.jhydrol.2014.11.025>
- Villalobos R, Retana J, Zúñiga B, Ríos A. 1997. Pronóstico de la precipitación total anual para la región Chorotega mediante un método de asociación de grupos de años. Informe Técnico No 5. Instituto Meteorológico Nacional, San José, Costa Rica.
- Vogt JV, Naumann G, Masante D, Spinoni J, Cammalleri C, Erian W, Pischke F, Pulwarty R, Barbosa P. 2018. Drought risk assessment and management: A conceptual framework. Joint Research Centre, European Commission. <https://doi.org/10.2760/057223>
- WMO. 2012. Standardized Precipitation Index User Guide. World Meteorological Organization, Geneva.
- Wolter K, Timlin MS. 1993. Monitoring ENSO in COADS with a seasonally adjusted principal component index. *Procedures of the 17th Climate Diagnostics Workshop*, Norman, 18-23 October, 52-57.
- Wolter K, Timlin MS. 1998. Measuring the strength of ENSO events – How does 1997/98 rank? *Weather* 53: 315-324. <https://doi.org/10.1002/j.1477-8696.1998.tb06408.x>
- Wu H, Svoboda MD, Hayes MJ, Wilhite DA, Wen F. 2007. Appropriate application of the standardized precipitation index in arid locations and dry seasons. *International Journal of Climatology* 27: 65-79. <https://doi.org/10.1002/joc.1371>

Supplementary material

Table SI. SPI values

2.0+	Extremely wet
1.5 to 1.99	Very wet
to 1.49	Moderately wet
-0.99 to 0.99	Near normal
-1.0 to -1.49	Moderately dry
-1.5 to -1.99	Severely dry
-2 and less	Extremely dry

Source: WMO (2012).